Electronic Supplementary Information (ESI)

Covalent switching, involving divinylbenzene ligands within 3D coordination polymers, indicated by changes in fluorescence

Ni-Ya Li,[ab] Dong Liu,[b] Brendan F. Abrahams[c] and Jian-Ping Lang*[a]

[a] College of Chemistry, Chemical Engineering and Materials Science, Soochow University, Suzhou 215123, P. R. China.

[b] College of Chemistry and Materials Science, Huaibei Normal University, Huaibei 235000, P. R. China.

[c] School of Chemistry, University of Melbourne, Victoria 3010, Australia.

Table of Contents

General procedures. All chemicals and reagents were purchased from TCI Co., Ltd., and Sigma-Aldrich Co. Powder XRD patterns were obtained using a PANalytical X'Pert PRO MPD system (PW3040/60). Thermal analysis was performed with a Perkin_Elmer TGA-7 thermogravimetric analyzer at a heating rate of 10 °C/min and a flow rate of 100 cm^3/min (N_2). ^1H NMR spectra were recorded at ambient temperature on a Bruker ADVANCE III (400MHz) spectrometer. ^1H NMR chemical shifts were referenced to the solvent signal in d_6-DMSO. Cross-polarization magic angle spinning (CPMAS) ^{13}C NMR spectra were recorded at a resonance frequency of 101.6 MHz on a BRUKER ADVANCE DSX 400 MHz spectrometer at ambient temperature. High-resolution mass spectra (HRMS) were obtained by electrospray ionization (ESI). Infrared (IR) samples were prepared as KBr pellets, and spectra were obtained in the 4000–400 cm^{-1} range using a Nicolet Avatar 360 FT-IR spectrophotometer. The elemental analyses for C, H and N were performed on an EA1110 CHNS elemental analyzer. The fluorescence spectra were obtained with a Perkin-Elmer LS55 spectrofluorometer. The confocal fluorescence microscopy images were taken with an Olympus FluoView FV 1000 confocal laser-scanning microscope.

Preparation of 1,4-bis[2-(3-pyridyl)ethenyl]benzene (3,3'-bpeb): A 50 mL round-bottom flask was charged with 1,4-diiodobenzene (3.29 g, 10 mmol), 3-vinylpyridine (2.73 g, 26 mmol), $PdCl_2(PPh_3)$ (0.35 g, 0.5 mmol) and triethylamine (3.03 g, 30 mmol) in 20 mL of DMF solution. The mixture was heated at 110 °C for a period of 20 h and then diluted with Et_2O (60 mL) to precipitate the product. The crude product was washed with a 0.1 M NaOH aqueous solution (50 mL) and distilled water and then dried in air. The product was collected as a yellow powder. Slow evaporation of a EtOH solution of this powder afforded yellow crystals of 3,3'-bpeb. Yield: 2.53 g (89%). Anal. calcd for $C_{20}H_{16}N_2$: C 84.48; H 5.67; N 9.85. Found: C 84.79; H 5.53; N 9.97. IR (KBr, cm^{-1}): 3019m, 1562s, 1505m, 1474m, 1423m, 1400s, 1331m, 1117m, 1019m, 964m, 878s,

828m, 805s, 706s, 622m, 574m, 519w, 455m. ^{1}H NMR (400 MHz, d_6-DMSO, 298 K, TMS): δ = 8.79 (d, J = 1.6 Hz, 2H), 8.46 (dd, J = 4.8, 1.2 Hz, 2H), 8.06 (d, J = 8.0 Hz, 2H), 7.67 (s, 4H), 7.40 (m, 6H).

Preparation of [Zn(1,4-NDC)(3,3'-bpeb)]$_n$ (1): To a 50 mL Teflon-lined autoclave was loaded $Zn(NO_3)_2{\cdot}6H_2O$ (0.298g, 1 mmol), 1,4-H_2ndc (0.216g, 1 mmol), 3,3'-bpeb (0.284g, 1 mmol) and H_2O (30 mL). The Teflon-lined autoclave was sealed and heated in an oven to 175°C for 60 h, and then cooled to ambient temperature at a rate of 5°C h^{-1} to form light-yellow crystals of **1**, which were washed with ethanol and dried in air. Yield: 0.484g (86% yield based on Zn). Anal. calcd. for $C_{32}H_{22}N_2O_4Zn$: C, 68.16; H, 3.93; N, 4.97. Found: C, 68.43; H, 3.87; N, 5.11. IR (KBr, cm^{-1}): 3079m, 1599s, 1571s, 1510m, 1457m, 1398s, 1359s, 1254m, 1125m, 1030w, 959s, 834s, 797s, 694m, 646m, 572m, 441w.

Preparation of [Zn(1,4-NDC)(3,3',3'',3'''-tppcp)$_{0.5}$]$_n$ (2): Single crystals of **1** (0.282 g) were irradiated by 30W LED lamp (λ = 365 nm) for about 4 h to form crystals of **2** in a quantitative yield (based on **1**). Anal. calcd. for $C_{32}H_{22}N_2O_4Zn$: C, 68.16; H, 3.93; N, 4.97. Found: C, 68.38; H, 4.01; N, 4.85. IR (KBr, cm^{-1}): 3081m, 1598s, 1569s, 1511m, 1457m, 1397s, 1359m, 1255m, 1124m, 1032w, 959s, 834s, 797s, 695m, 646m, 575m, 442w.

Isolation of 3,3',3'',3'''-tppcb: A mixture of $Na_2(H_2edta){\cdot}2H_2O$ (0.372 g), NaOH (0.088 g), **2** (0.141 g), H_2O (15 mL) and CH_2Cl_2 (25 mL) were placed in a 100 mL flask and stirred for 2 h. The organic phase was separated from the reaction mixture and the aqueous layers were extracted with CH_2Cl_2 (3 × 25 mL). The combined organic phase was concentrated to dryness in vacuo. The powder was then washed thoroughly with 0.1 M NaOH aqueous solution and H_2O, and finally dried with anhydrous Na_2SO_4 to give 3,3',3",3'"-tppcb as light-yellow powder. Yield: 56 mg (79%).

Anal. Calcd. for $C_{40}H_{32}N_4$: C 84.48, H 5.67, N 9.85; found: C 84.61, H 5.82, N 9.75. IR (KBr, cm^{-1}): 3025m, 1598s, 1551m, 1489w, 1416m, 1222m, 995m, 876s, 829m, 805s, 689m, 522w, 453m. ^{1}H NMR (400 MHz, d_6-DMSO): δ = 8.49 (d, *J* = 1.6 Hz, 4H), 8.27 (dd, *J* = 4.8, 1.2 Hz, 4H), 7.70 (d, *J* = 8.0 Hz, 4H), 7.21 (m, 8H), 6.70 (s, 4H), 4.79 (d, *J* = 6.4 Hz, 4H), 4.67 (d, *J* = 6.4 Hz, 4H).

Reversible conversion from 2 to 1: Single crystals of **2** (0.071 g) were heated in an oven to 260°C for 3 h to afford crystals of **1** in 100% yield based on **2**. Anal. calcd. for $C_{32}H_{22}N_2O_4Zn$: C, 68.16; H, 3.93; N, 4.97. Found: C, 68.03; H, 3.77; N, 4.79. IR (KBr, cm^{-1}): 3080m, 1599s, 1572s, 1511m, 1455m, 1398s, 1360m, 1255m, 1125m, 959s, 834s, 797s, 694m, 646m, 574m, 443w.

Preparation of $[Zn_2(3,3',4,4'\text{-bptc})(3,3'\text{-bpeb})]_n$ (3): To a 50 mL Teflon-lined autoclave was loaded $Zn(NO_3)_2{\cdot}6H_2O$ (0.596g, 2 mmol), 3,3',4,4'-H_4bptc (0.330g, 1 mmol), 3,3'-bpeb (0.284g, 1 mmol) and H_2O (30 mL). The Teflon-lined autoclave was sealed and heated in an oven to 175°C for 60 h, and then cooled to ambient temperature at a rate of 5°C h^{-1} to form light-yellow crystals of **3**, which were washed with ethanol and dried in air. Yield: 0.615g (83% yield based on Zn). Anal. calcd. for $C_{36}H_{22}N_2O_8Zn_2$: C, 58.32; H, 2.99; N, 3.78. Found: C, 58.18; H, 3.06; N, 3.93. IR (KBr, cm^{-1}): 3031m, 1595s, 1550s, 1488m, 1460m, 1404s, 1325m, 1264m, 1132m, 1097w, 961s, 839s, 782s, 701m, 670m, 572m, 442w.

Preparation of $[Zn_2(3,3',4,4'\text{-bptc})(3,3',3'',3'''\text{-bpbpvpcb})_{0.5}]_n$ (4): Single crystals of **3** (0.371 g) were irradiated by 30W LED lamp (λ = 365 nm) for about 3 h to form crystals of **4** in a quantitative yield (based on **3**). Anal. calcd. for $C_{36}H_{22}N_2O_8Zn_2$: C, 58.32; H, 2.99; N, 3.78. Found: C, 58.49; H, 2.86; N, 3.95. IR (KBr, cm^{-1}): 3035m, 1596s, 1549s, 1490m, 1459m, 1404s, 1324m, 1268m, 1157m, 1097w, 975s, 842s, 786s, 703m, 671m, 573m, 441w.

Isolation of 3,3',3'',3'''-bpbpvpcb: A mixture of $Na_2(H_2edta)\cdot 2H_2O$ (0.372 g), NaOH (0.088 g), **4** (0.148 g), H_2O (15 mL) and CH_2Cl_2 (25 mL) were placed in a 100 mL flask and stirred for 2 h. The organic phase was separated from the reaction mixture and the aqueous layers were extracted with CH_2Cl_2 (3 x 25 mL). The combined organic phase was concentrated to dryness in vacuo. The powder was then washed thoroughly with 0.1 M NaOH aqueous solution and H_2O, and finally dried with anhydrous Na_2SO_4 to give 3,3',3",3'''-bpbpvpcb as light-yellow powder. Yield: 43 mg (76%). Anal. Calcd. for $C_{40}H_{32}N_4$: C 84.48, H 5.67, N 9.85; found: C 84.42, H 5.79, N 9.74. IR (KBr, cm^{-1}): 3025m, 1567s, 1512s, 1478m, 1420s, 1315m, 1261m, 1181w, 1098m, 929m, 865m, 821s, 707s, 553m, 455m. ^{1}H NMR (400 MHz, d_6-DMSO): δ = 8.72 (d, J = 1.6 Hz, 2H), 8.43 (m, 4H), 8.25 (dd, J = 4.8, 1.2 Hz, 2H), 7.99 (d, J = 8.0 Hz, 2H), 7.66 (t, 2H), 7.42 (d, J = 8.4 Hz, 4H), 7.37 (dd, J = 8.0, 4.8 Hz, 2H), 7.27 (t, 6H), 7.18 (m, 4H), 4.64 (dd, J = 6.8, 4.4 Hz, 4H).

Reversible conversion from 4 to 3: Single crystals of **4** (0.074 g) were heated in an oven to 260°C for 3 h to afford crystals of **3** in 100% yield based on **4**. Anal. calcd. for $C_{36}H_{22}N_2O_8Zn_2$: C, 58.32; H, 2.99; N, 3.78. Found: C, 58.21; H, 2.84; N, 3.66. IR (KBr, cm^{-1}): 3031m, 1596s, 1549s, 1488m, 1461m, 1404s, 1326m, 1264m, 1133m, 961s, 829s, 782s, 700m, 669m, 573m, 440w.

X-ray diffraction crystallography. All measurements were collected on a Bruker SMART APEX II CCD diffractometer equipped with graphite-monochromated Mo-Kα (λ = 0.71073 Å) by using the Φ/ω scan technique. Absorption correction was based on symmetry equivalent reflections using the SADABS program. Single crystals of 3,3'-bpeb, **1**, **2**, **3** and **4** suitable for X-ray analysis were obtained directly from the above preparations. All crystal structures were solved by direct methods and refined on F^2 by full-matrix least-squares methods with the *SHELXL-2014* program.[S1] All non-hydrogen atoms refined anisotropically. All H atoms were introduced at the calculated positions and included in the structure-factor calculations.

Table S1 Crystal data and structure refinement parameters for 3,3'-bpeb, **1**, **2**, **3** and **4.**

Compounds	3,3'-bpeb	**1**	**2**	**3**	**4**
Formula	$C_{20}H_{16}N_2$	$C_{32}H_{22}N_2O_4Zn$	$C_{32}H_{22}N_2O_4Zn$	$C_{36}H_{22}N_2O_8Zn_2$	$C_{36}H_{22}N_2O_8Zn_2$
Formula weight	284.35	563.91	563.91	741.34	741.34
Crystal system	monoclinic	monoclinic	monoclinic	triclinic	triclinic
Space group	$P2_1/n$	$P2_1/n$	$P2_1/n$	$P\bar{1}$	$P\bar{1}$
a/Å	11.883(2)	10.553(2)	10.923(2)	10.324(2)	10.502(2)
b/Å	6.3386(13)	13.677(3)	13.139(3)	12.009(2)	11.871(2)
c/Å	20.211(4)	17.241(3)	17.004(3)	13.220(3)	13.571(3)
α/°				94.44(3)	94.67(3)
β/°	92.61(3)	93.47(3)	94.47(3)	111.17(3)	108.33(3)
γ/°				97.20(3)	104.03(3)
V/Å^3	1520.8(5)	2483.9(8)	2433.0(8)	1503.0(6)	1535.1(7)
Z	4	4	4	2	2
D_c/(g·cm^{-3})	1.242	1.508	1.539	1.638	1.604
F(000)	600	1160	1160	752	752
μ (Mo Kα, mm^{-1})	0.073	1.032	1.054	1.656	1.622
Total reflections.	26359	44964	18247	28293	23881
Unique reflections.	3507	5715	4245	6893	7027
No. of parameters	199	352	334	433	433
R^a	0.0575	0.0319	0.0770	0.0313	0.0527
$R_w{}^b$	0.1359	0.0836	0.1973	0.0865	0.1071
GOF^c	1.036	1.062	1.097	1.022	1.007
CCDC number	1824665	1824666	1824667	1824668	1824669

$^aR = \sum||F_o|-|F_c||/\sum|F_o|$. $^bwR = \{\sum w(F_o^2-F_c^2)^2/\sum w(F_o^2)^2\}^{1/2}$. $^cGOF = \{\sum w[(F_o^2-F_c^2)^2]/(n-p)\}^{1/2}$, where n is the number of reflections and p is total number of parameters refined.

Crystal data for the regenerated sample of **1** from **2** upon heating at 260°C: monoclinic, space group $P2_1/n$, a = 10.503(3), b = 13.686(5), c = 17.275(6) Å, β = 93.496(12)°, V = 2478.6(14) Å^3, which are almost the same as those of **1**, implying the reversible SCSC transformation from **2** to **1**.

Crystal data for the regenerated sample of **3** from **4** upon heating at 260°C: triclinic, space group $P\bar{1}$, a = 10.333(2), b = 12.014(2), c = 13.235(3) Å, α = 94.49(3)°, β = 111.12(3)°, γ = 97.28(3)°, V = 1506.6(6) Å^3. which are almost the same as those of **3**, implying the reversible SCSC transformation from **4** to **3**.

Table S2 Selected bond lengths (Å) and angles (º) for **1-4**.

Compound **1**

Zn(1)-O(3A)	2.0371(12)	Zn(1)-O(4B)	2.0796(13)
Zn(1)-O(1)	2.1524(15)	Zn(1)-N(2C)	2.1695(17)
Zn(1)-N(1)	2.1721(17)	Zn(1)-O(2)	2.2763(14)
O(3A)-Zn(1)-O(4B)	116.10(5)	O(3A)-Zn(1)-O(1)	156.22(5)
O(4B)-Zn(1)-O(1)	87.36(5)	O(3A)-Zn(1)-N(2C)	90.49(6)
O(4B)-Zn(1)-N(2C)	92.98(6)	O(1)-Zn(1)-N(2C)	92.15(6)
O(3A)-Zn(1)-N(1)	85.75(6)	O(4B)-Zn(1)-N(1)	88.48(6)
O(1)-Zn(1)-N(1)	91.39(6)	N(2C)-Zn(1)-N(1)	176.23(6)
O(3A)-Zn(1)-O(2)	97.73(5)	O(4B)-Zn(1)-O(2)	145.66(5)
O(1)-Zn(1)-O(2)	58.55(5)	N(2C)-Zn(1)-O(2)	92.37(6)
N(1)-Zn(1)-O(2)	88.37(6)		

Compound **2**

Zn(1)-O(3A)	2.069(4)	Zn(1)-O(4B)	2.116(5)
Zn(1)-N(1)	2.142(5)	Zn(1)-N(2C)	2.145(6)
Zn(1)-O(2)	2.226(5)	Zn(1)-O(1)	2.238(4)
O(3A)-Zn(1)-O(4B)	115.36(17)	O(3A)-Zn(1)-N(1)	91.39(19)
O(4B)-Zn(1)-N(1)	91.8(2)	O(3A)-Zn(1)-N(2C)	89.72(19)
O(4B)-Zn(1)-N(2C)	85.4(2)	N(1)-Zn(1)-N(2C)	177.2(2)
O(3A)-Zn(1)-O(2)	153.97(18)	O(4B)-Zn(1)-O(2)	90.56(17)

N(1)-Zn(1)-O(2)	90.03(19)	N(2C)-Zn(1)-O(2)	90.08(19)
O(3A)-Zn(1)-O(1)	95.66(17)	O(4B)-Zn(1)-O(1)	148.68(16)
N(1)-Zn(1)-O(1)	91.57(19)	N(2C)-Zn(1)-O(1)	90.8(2)
O(2)-Zn(1)-O(1)	58.31(16)		

Compound **3**

Zn(1)-O(6A)	1.9614(17)	Zn(1)-O(7B)	1.9655(19)
Zn(1)-O(1)	2.0282(15)	Zn(1)-N(1)	2.035(2)
Zn(2)-O(1)	1.9678(15)	Zn(2)-O(3C)	2.0008(18)
Zn(2)-O(5A)	2.0026(18)	Zn(2)-N(2D)	2.035(2)
Zn(2)-O(4C)	2.410(2)		
O(6A)-Zn(1)-O(7B)	13.61(8)	O(6A)-Zn(1)-O(1)	100.63(7)
O(7B)-Zn(1)-O(1)	127.19(7)	O(6A)-Zn(1)-N(1)	100.13(8)
O(7B)-Zn(1)-N(1)	100.63(8)	O(1)-Zn(1)-N(1)	111.85(8)
O(1)-Zn(2)-O(3C)	138.89(8)	O(1)-Zn(2)-O(5A)	102.70(7)
O(3C)-Zn(2)-O(5A)	103.54(8)	O(1)-Zn(2)-N(2D)	105.58(7)
O(3C)-Zn(2)-N(2D)	104.14(8)	O(5A)-Zn(2)-N(2D)	92.81(8)
O(1)-Zn(2)-O(4C)	96.19(7)	O(3C)-Zn(2)-O(4C)	58.22(7)
O(5A)-Zn(2)-O(4C)	80.39(8)	N(2D)-Zn(2)-O(4C)	158.15(7)

Compound **4**

Zn(1)-O(2)	1.951(3)	Zn(1)-O(3A)	1.996(3)
Zn(1)-N(2B)	2.049(3)	Zn(1)-O(6C)	2.056(3)

Zn(2)-O(6C)	1.971(2)	Zn(2)-O(1)	2.010(3)
Zn(2)-O(7D)	2.020(3)	Zn(2)-N(1)	2.030(3)
Zn(2)-O(8D)	2.397(3)		
O(2)-Zn(1)-O(3A)	107.54(14)	O(2)-Zn(1)-N(2B)	106.06(13)
O(3A)-Zn(1)-N(2B)	105.61(14)	O(2)-Zn(1)-O(6C)	101.16(12)
O(3A)-Zn(1)-O(6C)	132.35(14)	N(2B)-Zn(1)-O(6C)	101.79(12)
O(6C)-Zn(2)-O(1)	97.51(11)	O(6C)-Zn(2)-O(7D)	142.67(13)
O(1)-Zn(2)-O(7D)	108.99(13)	O(6C)-Zn(2)-N(1)	106.52(12)
O(1)-Zn(2)-N(1)	91.47(13)	O(7D)-Zn(2)-N(1)	98.78(13)
O(6C)-Zn(2)-O(8D)	102.04(11)	O(1)-Zn(2)-O(8D)	81.66(12)
O(7D)-Zn(2)-O(8D)	58.22(12)	N(1)-Zn(2)-O(8D)	151.26(12)

Symmetry codes: (**1**) A: $x + 1/2, - y + 3/2, z - 1/2$. B: $- x + 1/2, y - 1/2, - z + 3/2$. C: $x - 1, y - 1, z$. (**2**) A: $x + 1/2, - y + 1/2, z - 1/2$. B: $- x + 1/2, y + 1/2, - z + 3/2$. C: $x + 1, y - 1, z$. (**3**) A: $x, y + 1, z$. B: $- x + 2, - y, - z$. C: $- x + 2, - y + 1, - z + 1$. D: $x - 1, y - 1, z - 1$. (**4**) A: $- x + 1, - y + 1, - z + 1$. B: $x - 1, y - 1, z - 1$. C: $x, y + 1, z$. D: $- x + 1, - y, - z$.

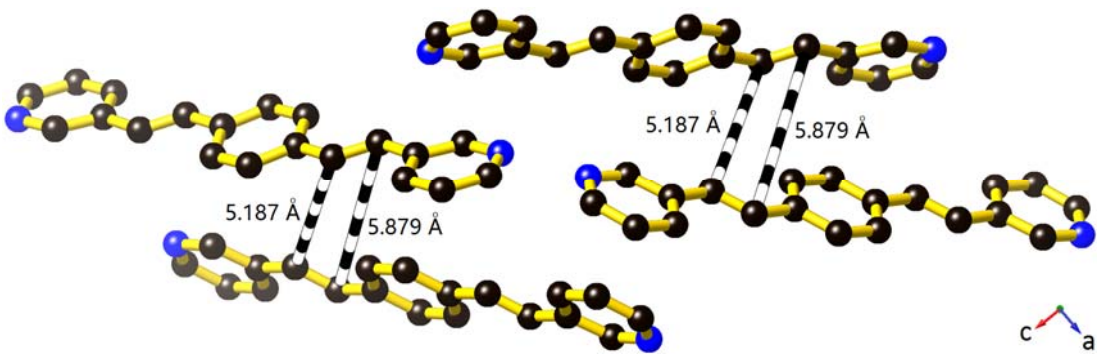

Fig. S1 The crystal structure of pure 3,3'-bpeb.

Noted: As shown in Fig. S1, the olefinic bonds of adjacent 3,3'-bpeb ligands in the crystal lattice are not parallel aligned and the distances between the nearest neighbor olefinic bonds are 5.187 or 5.880 Å. Such an arrangement of 3,3'-bpeb molecules does not satisfy Schmidt's topochemical criterion for a photochemical [2+2] cycloaddition reaction.[S2] The similar ^{1}H NMR spectra of 3,3'-bpeb before and after UV irradiation also confirm that 3,3'-bpeb is photo-inert (Fig. S2).

(a)

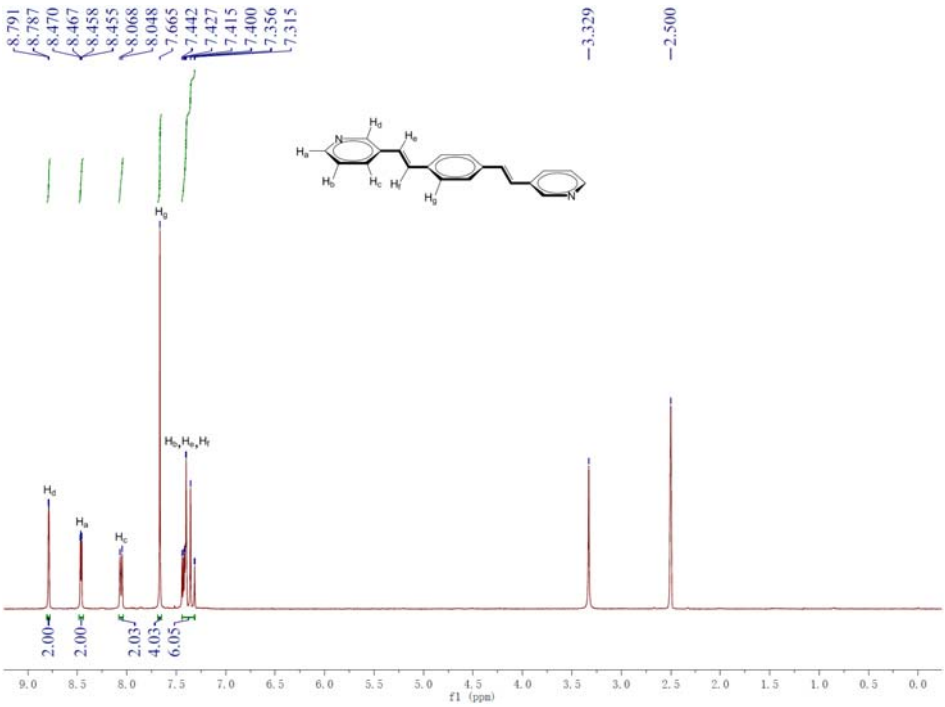

(b)

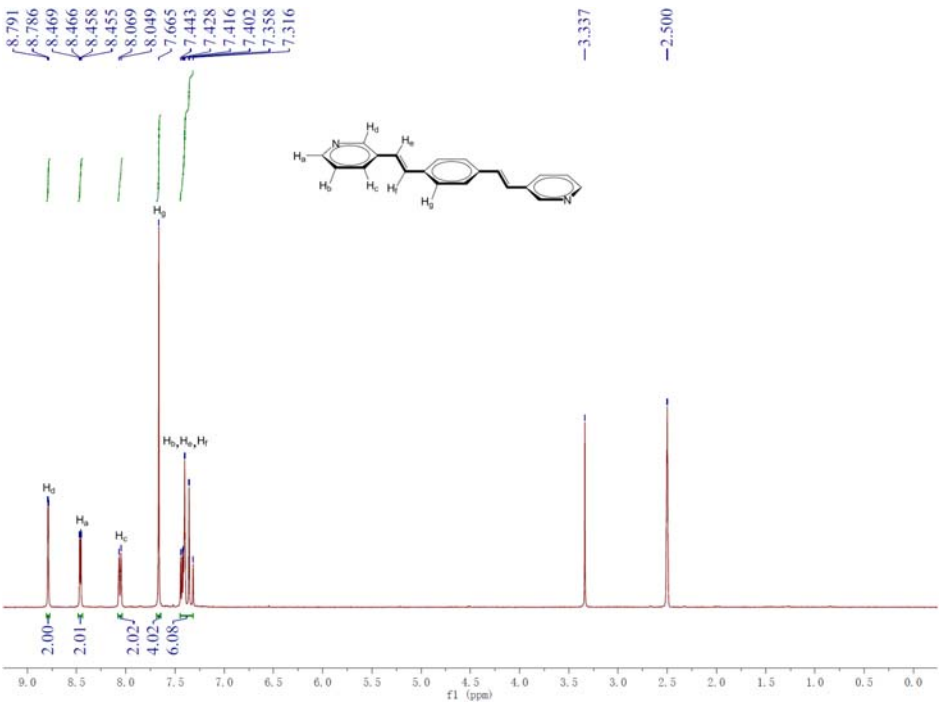

Fig. S2 (a) The ^{1}H NMR spectrum of 3,3'-bpeb. (b) The ^{1}H NMR spectrum of 3,3'-bpeb after UV irradiation for 12h. Deuterated solvent: d_6-DMSO.

Noted: The ^{1}H NMR spectra of 3,3'-bpeb before and after UV irradiation are similar, suggesting that 3,3'-bpeb is photo-inert.

(a) (b)

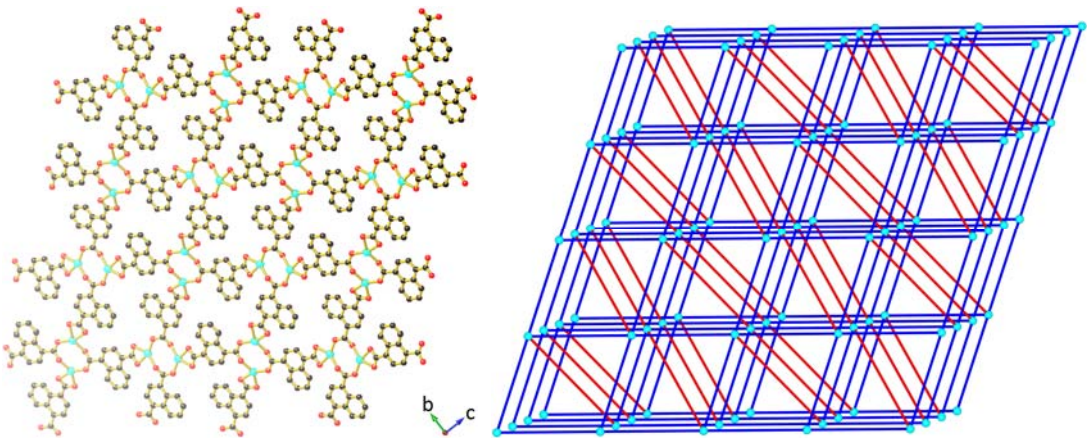

Fig. S3 (a) View of the 2D $[Zn(1,4\text{-ndc})]_n$ network in **1**. The cyan, red and black balls represent Zn, O and C atoms, respectively. (b) View of the topological net of **1**.

(a)

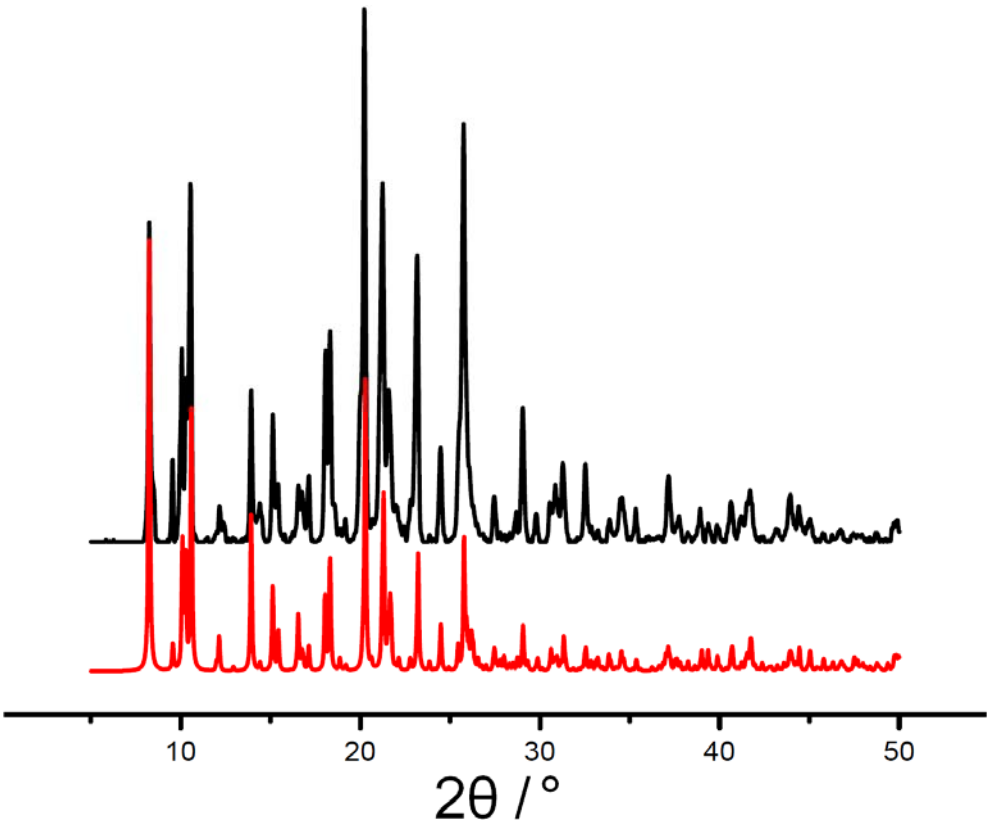

(b)

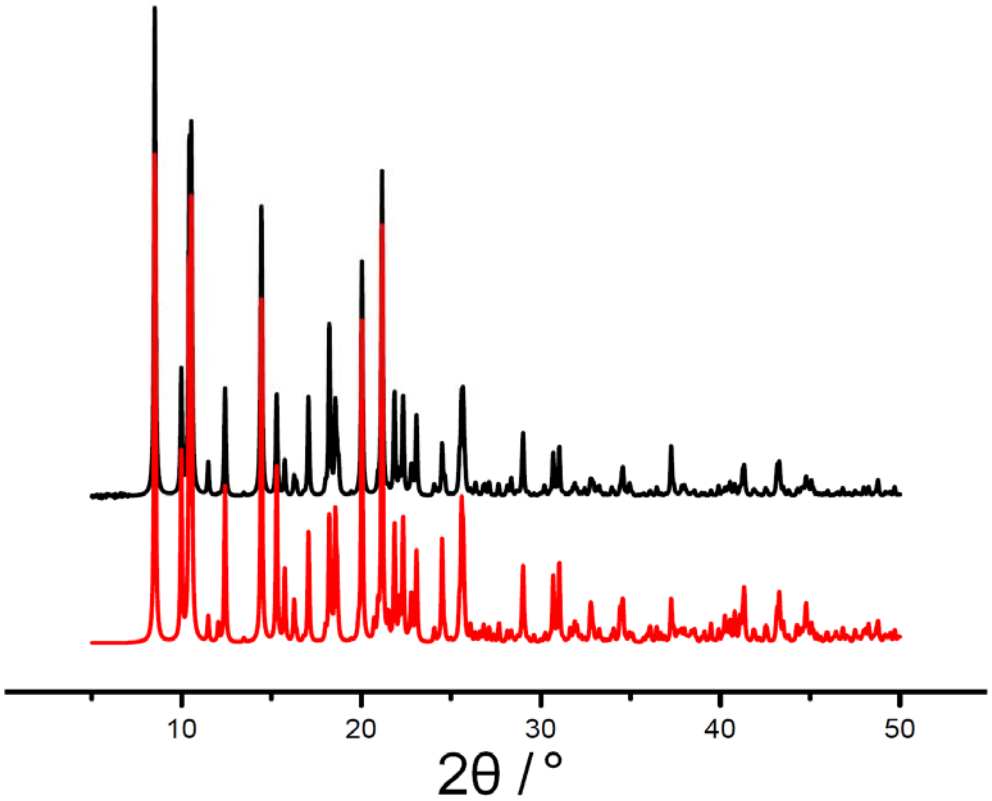

(c)

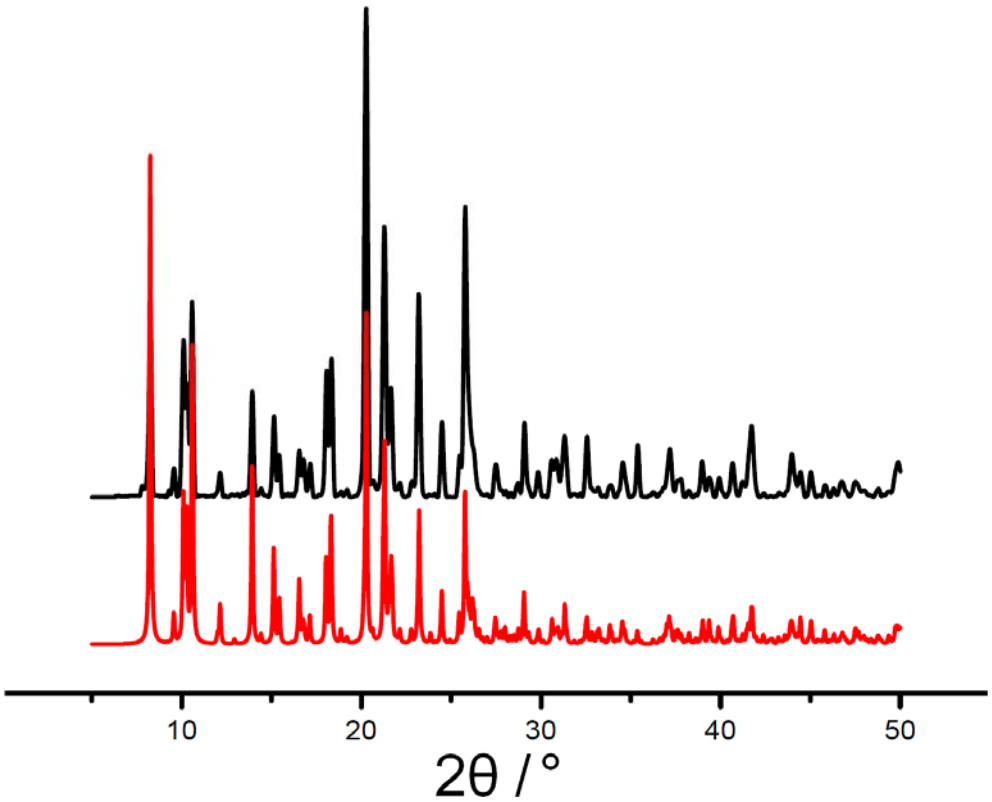

(d)

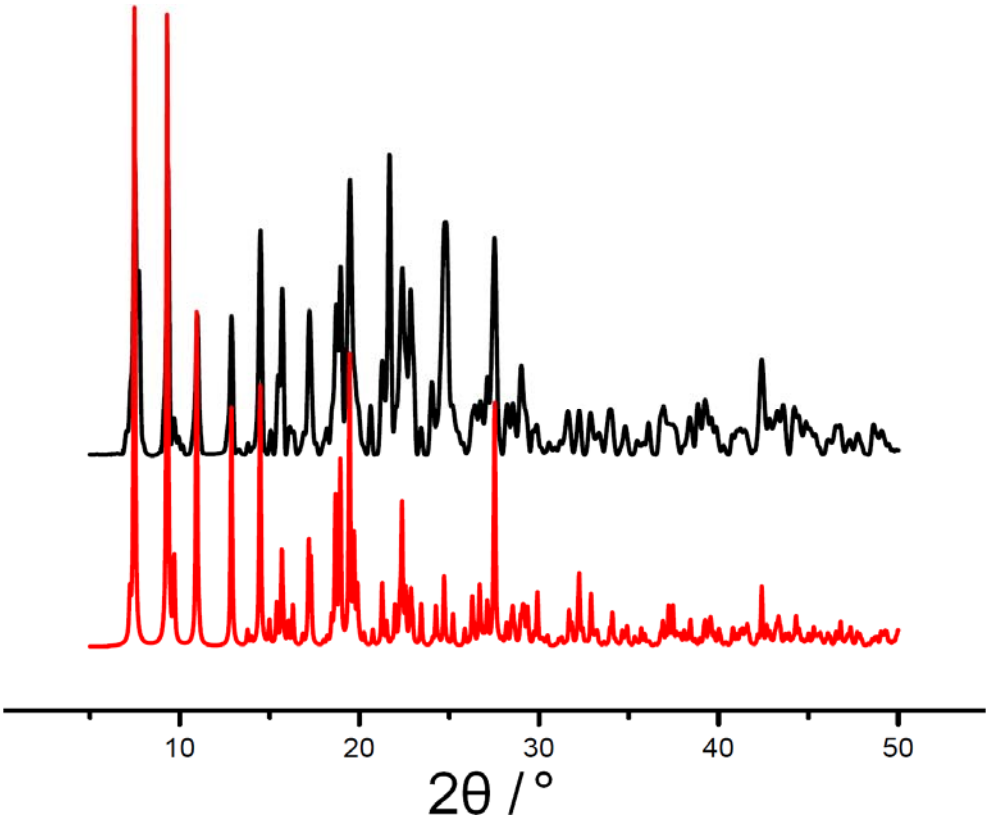

(e)

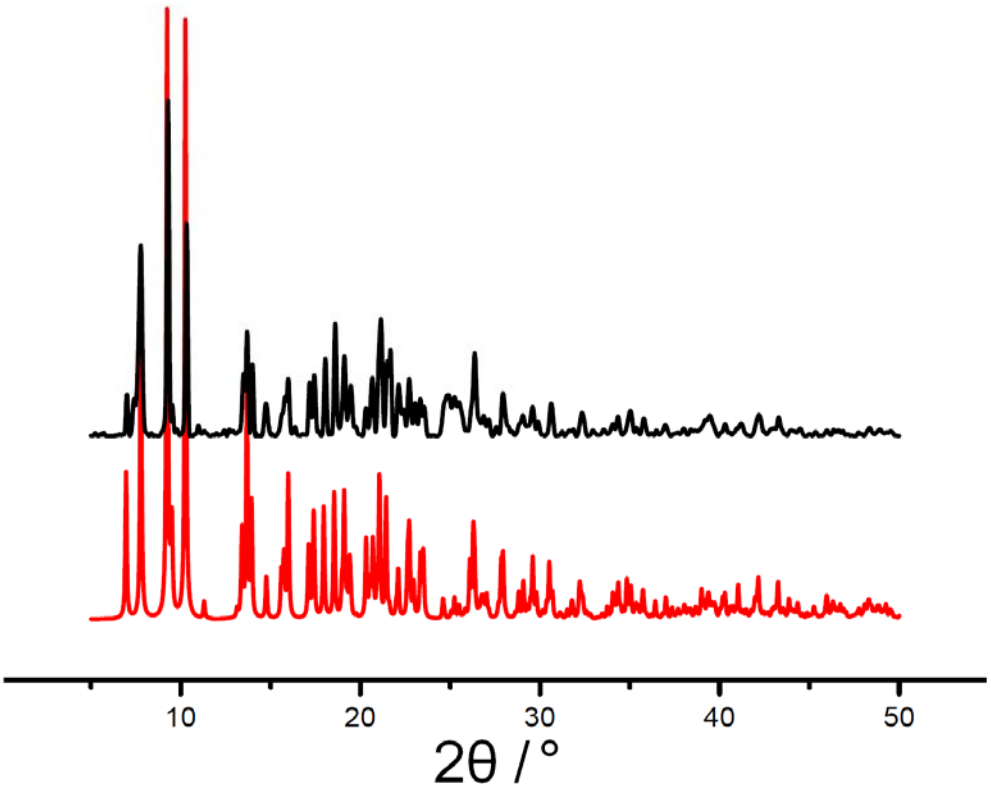

(f)

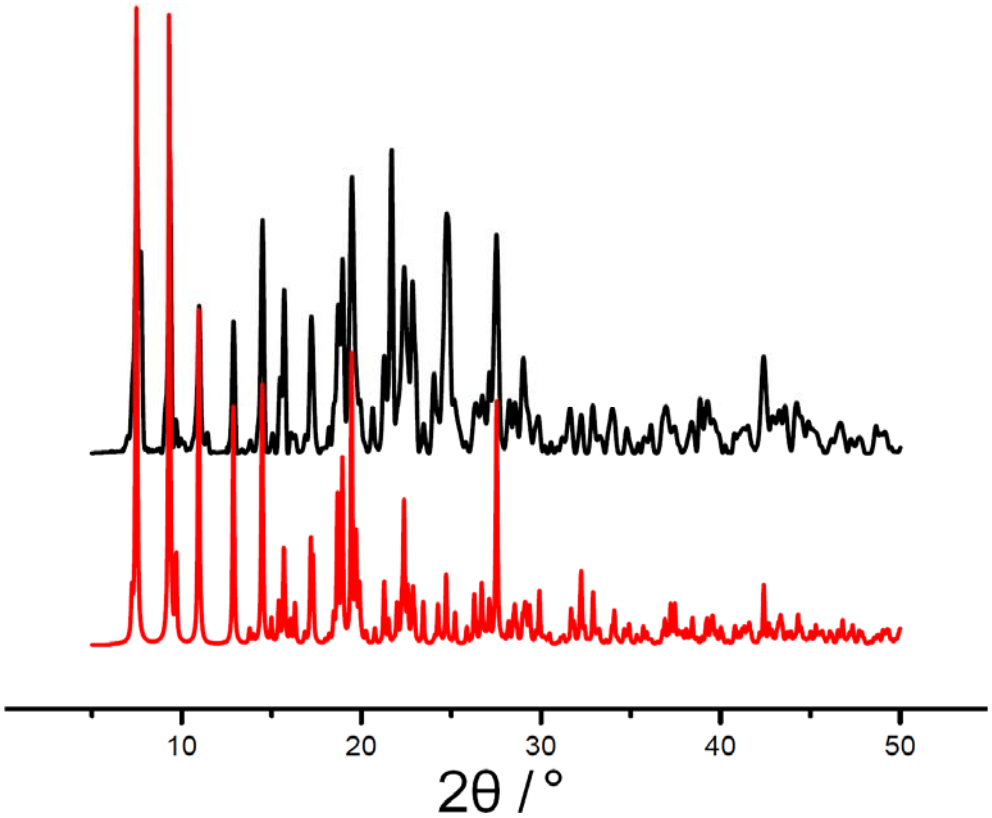

Fig. S4 (a) PXRD patterns of **1** (from single crystal data: red; as-synthesis: black). (b) PXRD patterns of **2** (from single crystal data: red; as-synthesis: black). (c) PXRD patterns of **1** (from single crystal data: red) and the sample of **2** after heating (black). (d) PXRD patterns of **3** (from single crystal data: red; as-synthesis: black). (e) PXRD patterns of **4** (from single crystal data: red; as-synthesis: black). (f) PXRD patterns of **3** (from single crystal data: red) and the sample of **4** after heating (black).

Noted: Figures S2c and S2f confirmed the reversible structural transformations from **2** to **1** and **4** to **3**, respectively.

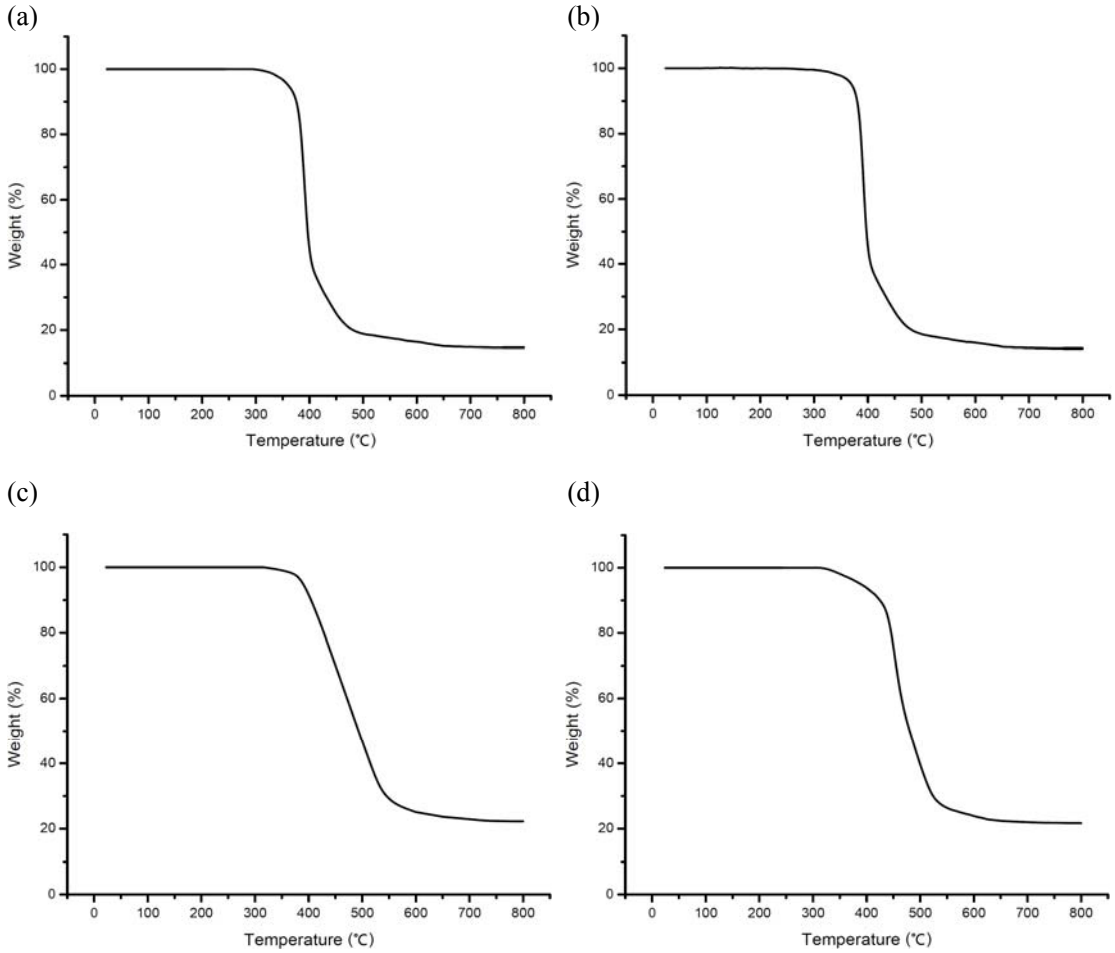

Fig. S5 The TGA curves for **1** (a), **2** (b), **3** (c) and **4** (d).

Noted: The TGA curve of **1** shows that its framework is stable up to 300 °C. Beyond this temperature, its framework began to get decomposed. The remaining weight of 14.68% is in accordance with the ZnO residue (calcd. 14.43%). **2** exhibits stability up to 299 °C followed by decomposition with a weight loss. Finally, the remaining residue is presumed to be ZnO (obsd 14.21%, calcd. 14.43%). Compound **3** is stable up to about 312°C upon at which temperature decomposition is observed. The TGA curve of **4** is similar to that of **3**. The final residues of **3** and **4** were assumed to be ZnO (ca. 21.96%), which is consistent with the experimental weights of residues (22.23% for **3** and 21.68% for **4**).

(a) (b)

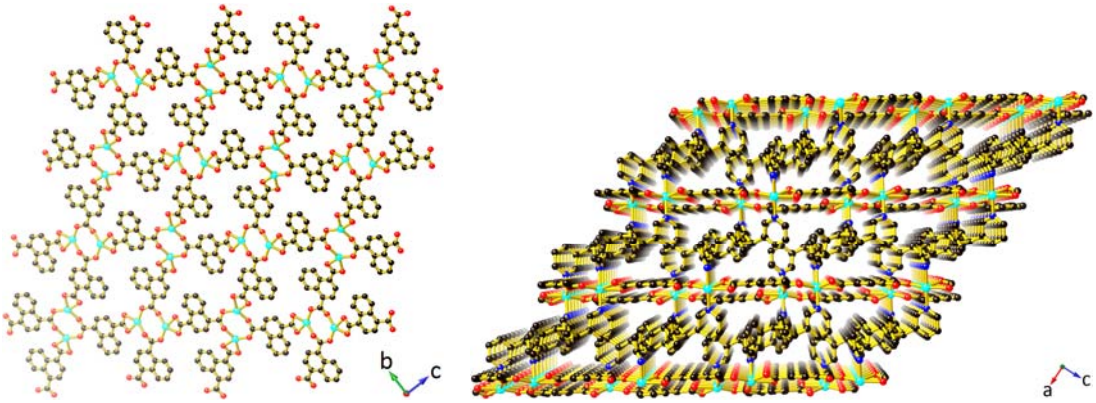

(c)

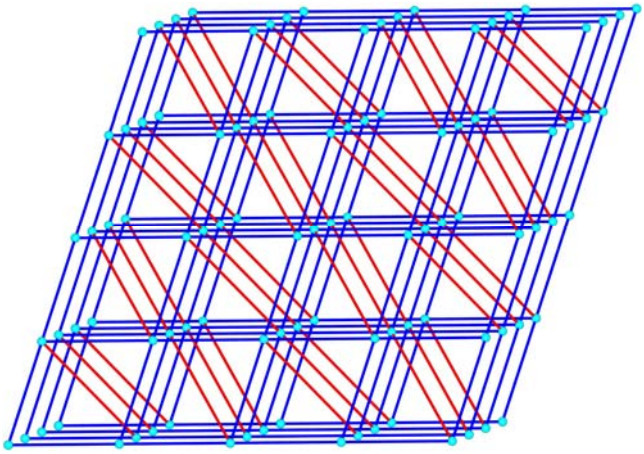

Fig. S6 (a) View of the 2D $[Zn(1,4\text{-ndc})]_n$ network in **2**. (b) View of the 3D framework of **2** along the *b* axis. The cyan, blue, red and black balls represent Zn, N, O and C atoms, respectively. (c) View of the topological net of **2**.

(a)

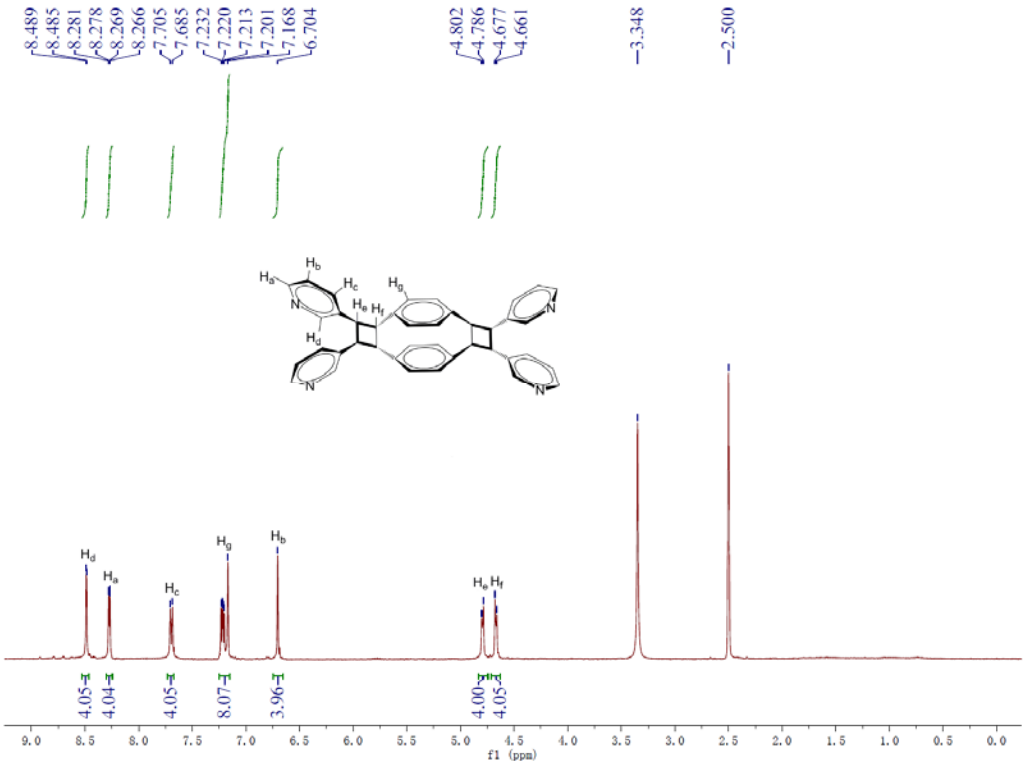

(b)

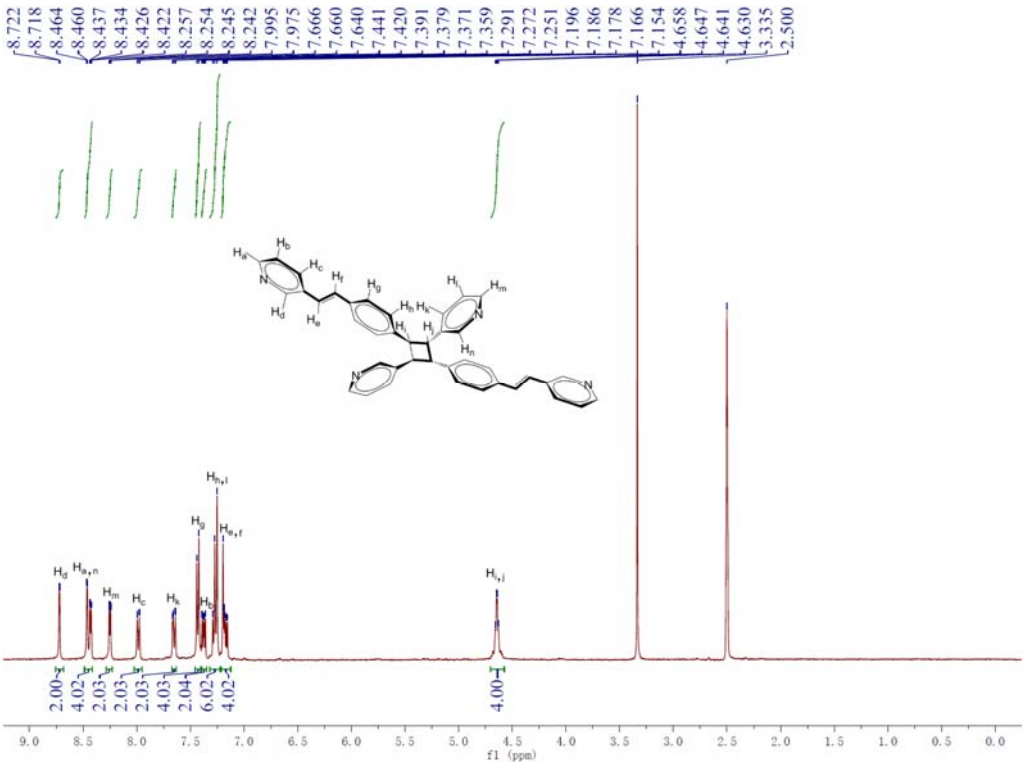

Fig. S7 (a) The ^{1}H NMR spectrum of 3,3',3",3'''-tppcb. (b) The ^{1}H NMR spectrum of 3,3',3",3'''-bpbpvpcb. Deuterated solvent: d_6-DMSO.

(a)

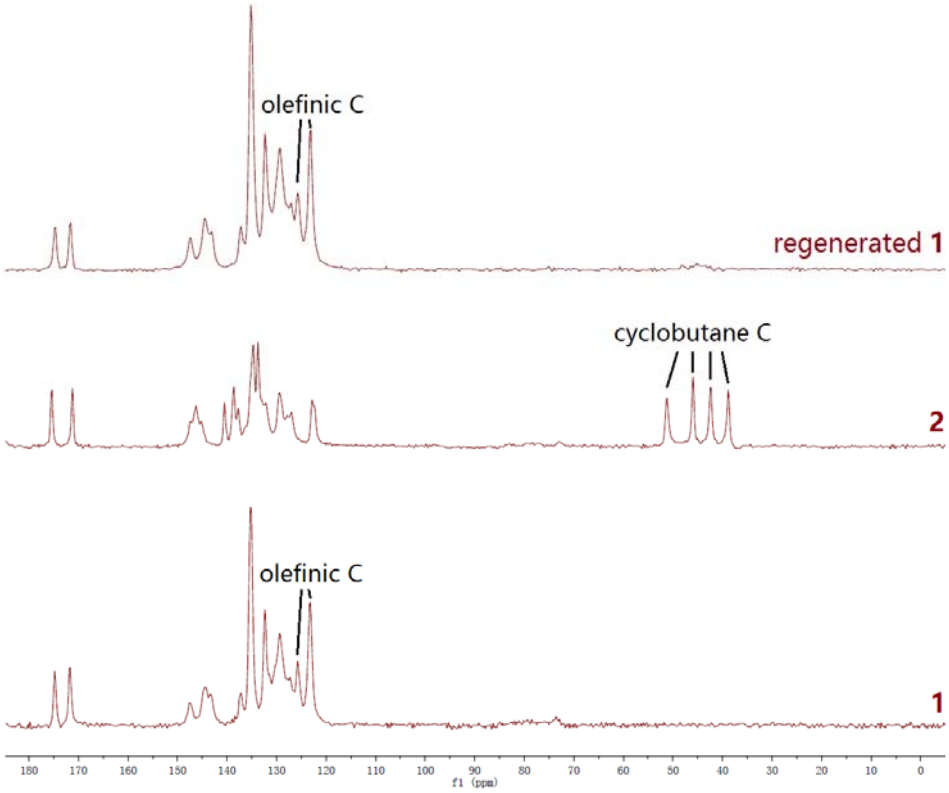

(b)

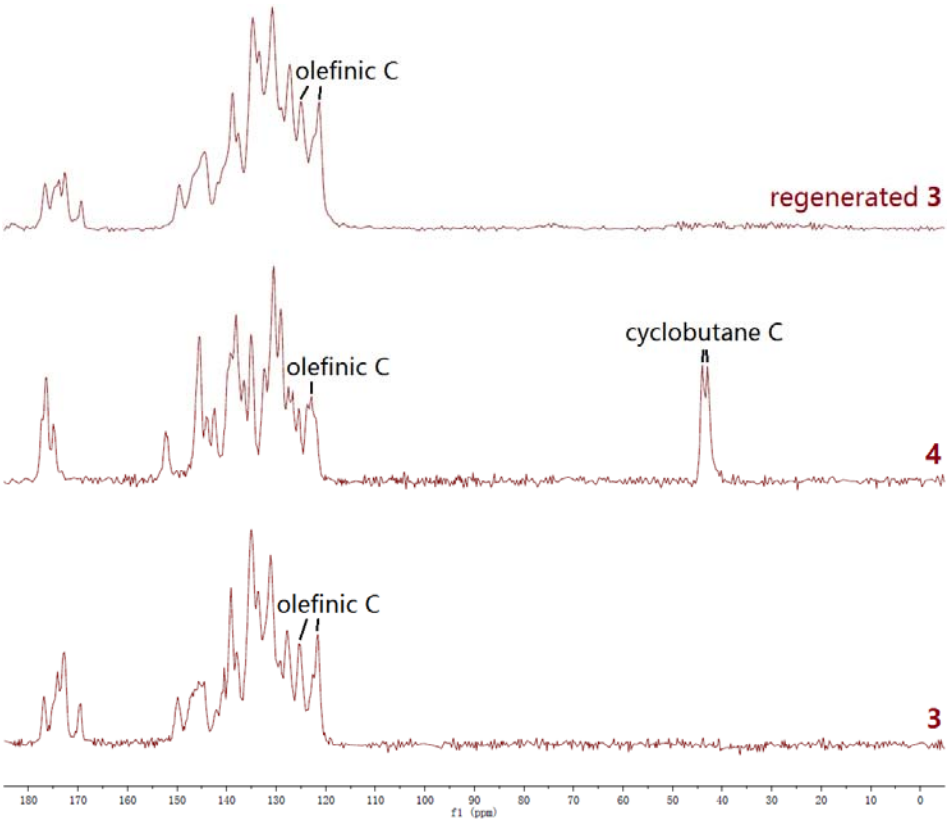

Fig. S8 (a) The CPMAS ^{13}C NMR spectra of **1, 2** and regenerated **1**. (b) The CPMAS ^{13}C NMR spectra of **3, 4** and regenerated **3**.

(a)

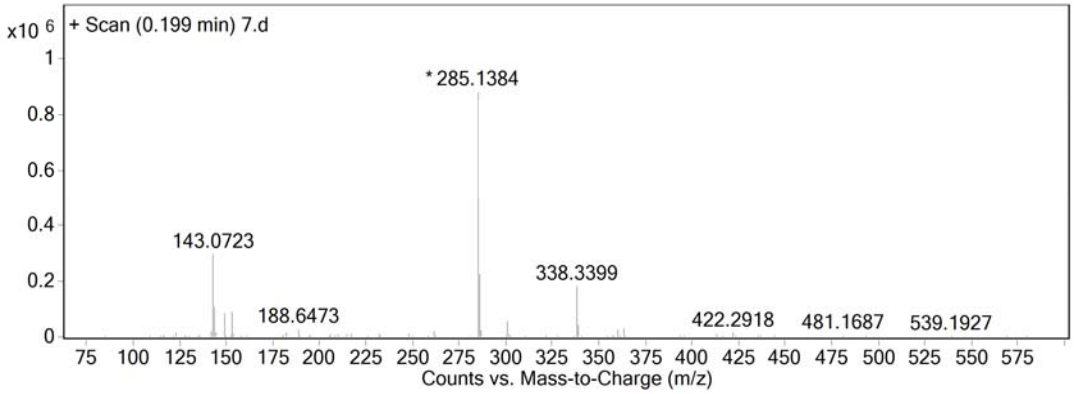

(b)

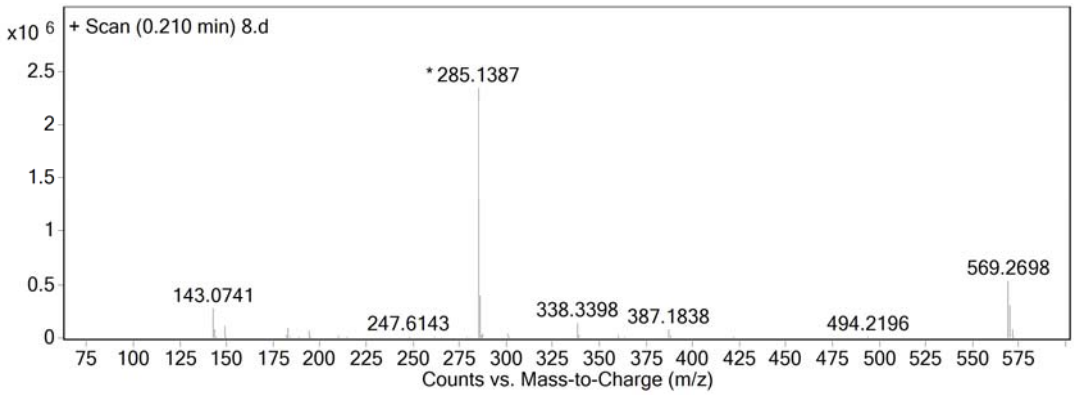

(c)

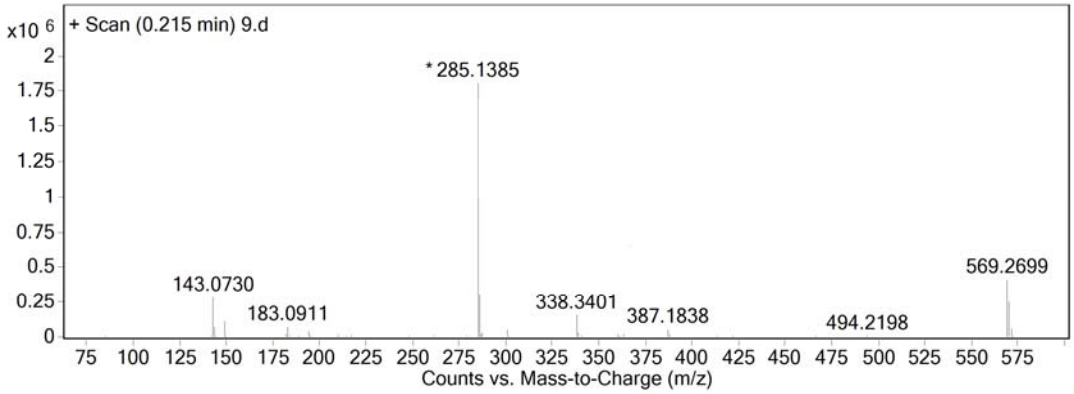

Fig. S9 HRMS Spectra of 3,3'-bpeb (a), 3,3',3",3'"-tppcb (b) and 3,3',3",3'"-bpbpvpcb (c).

(a)

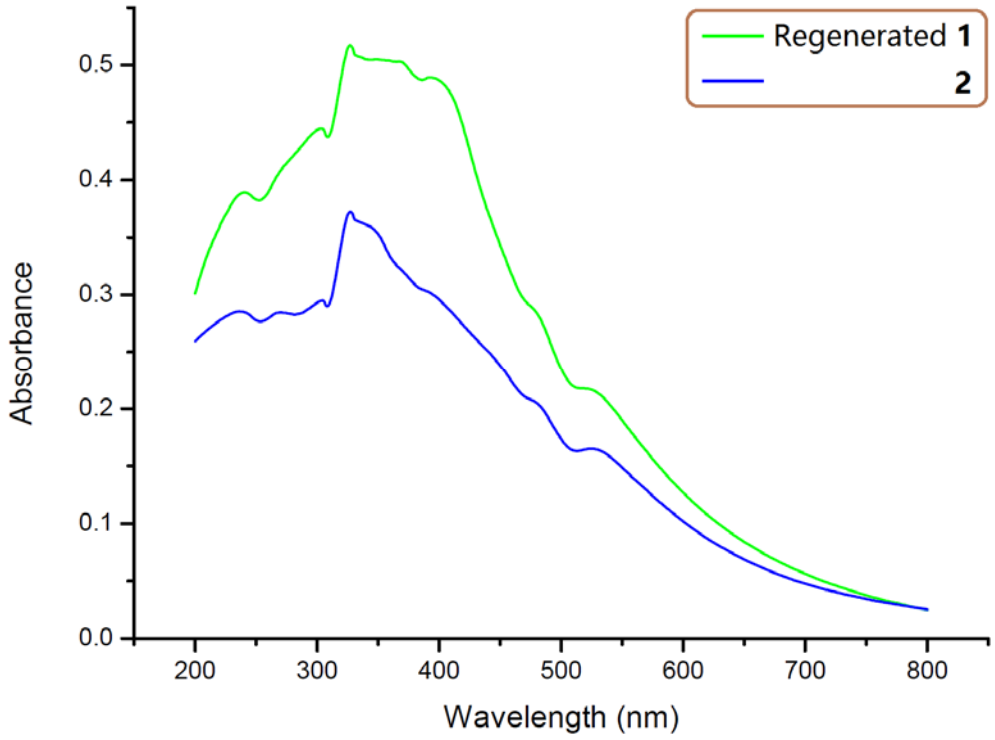

(b)

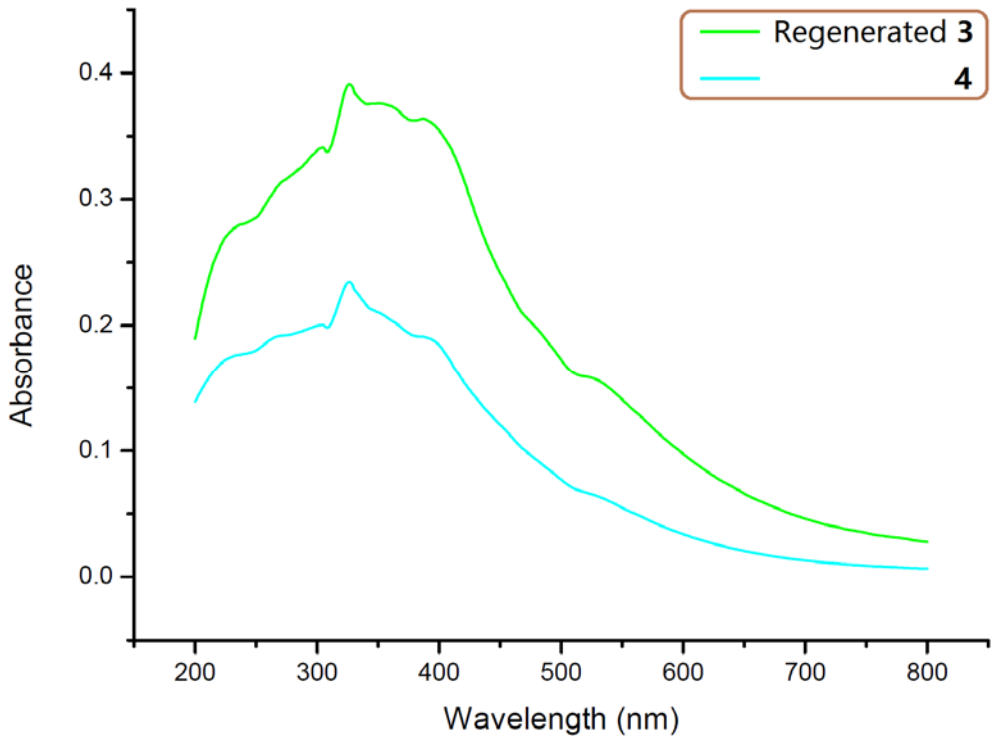

Fig. S10 (a) Solid-state optical absorbance spectra of **2** and regenerated **1** derived from diffuse reflectance data. (b) Solid-state optical absorbance spectra of **4** and regenerated **3** derived from diffuse reflectance data.

(a)

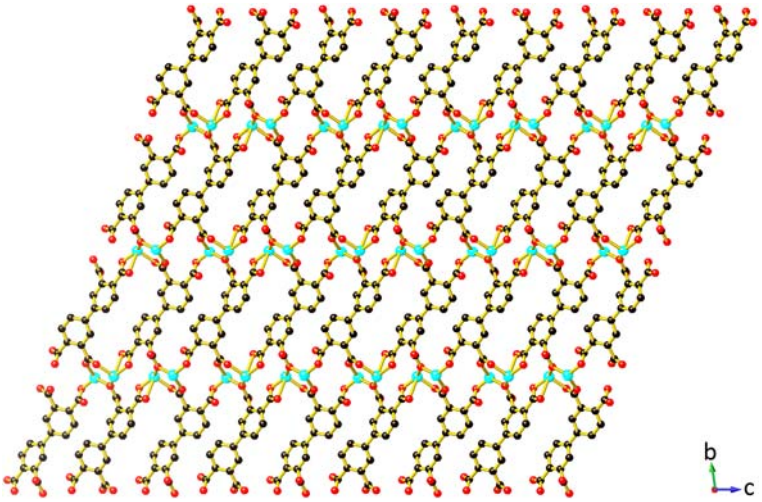

(b)

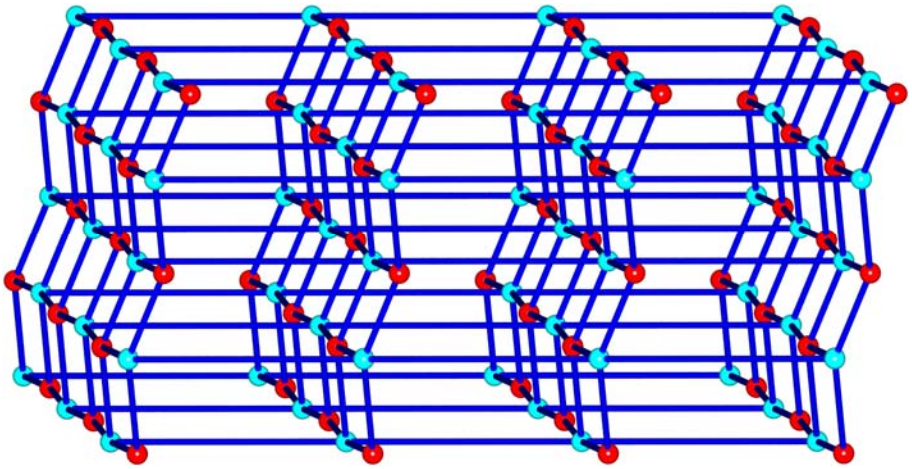

Fig. S11 (a) View of the 2D $[Zn_2(3,3',4,4'\text{-bptc})]_n$ network in **3**. The cyan, red and black balls represent Zn, O and C atoms, respectively. (b) View of the topological net of **3**.

(a)

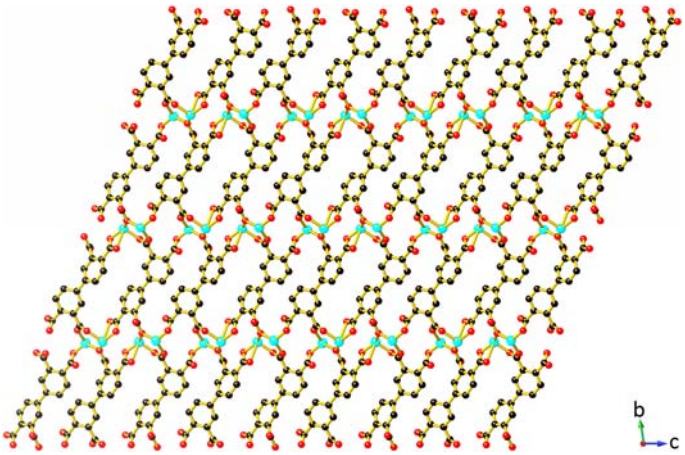

(b)

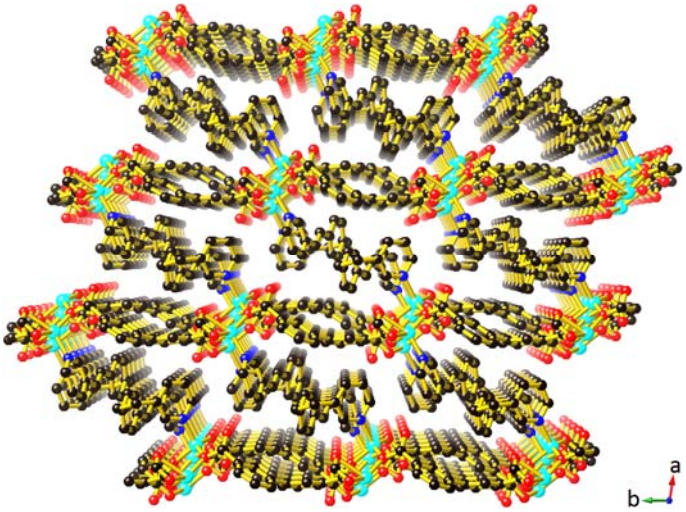

(c)

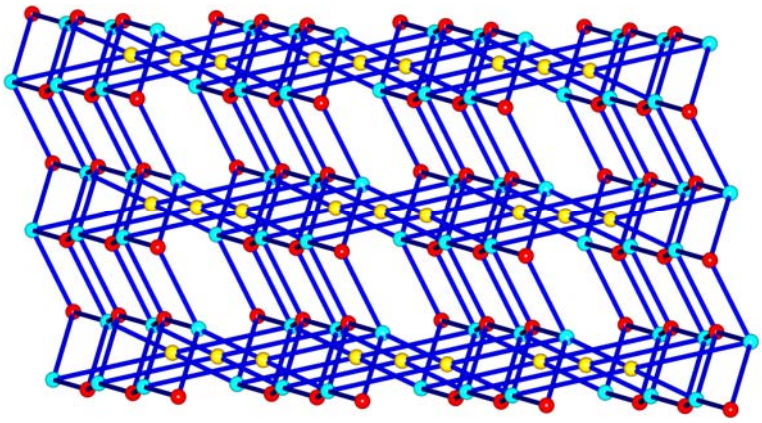

Fig. S12 (a) View of the 2D $[Zn_2(3,3',4,4'\text{-bptc})]_n$ network in **4**. (b) View of the 3D framework of **4**. The cyan, blue, red and black balls represent Zn, N, O and C atoms, respectively. (c) View of the topological net of **4**.

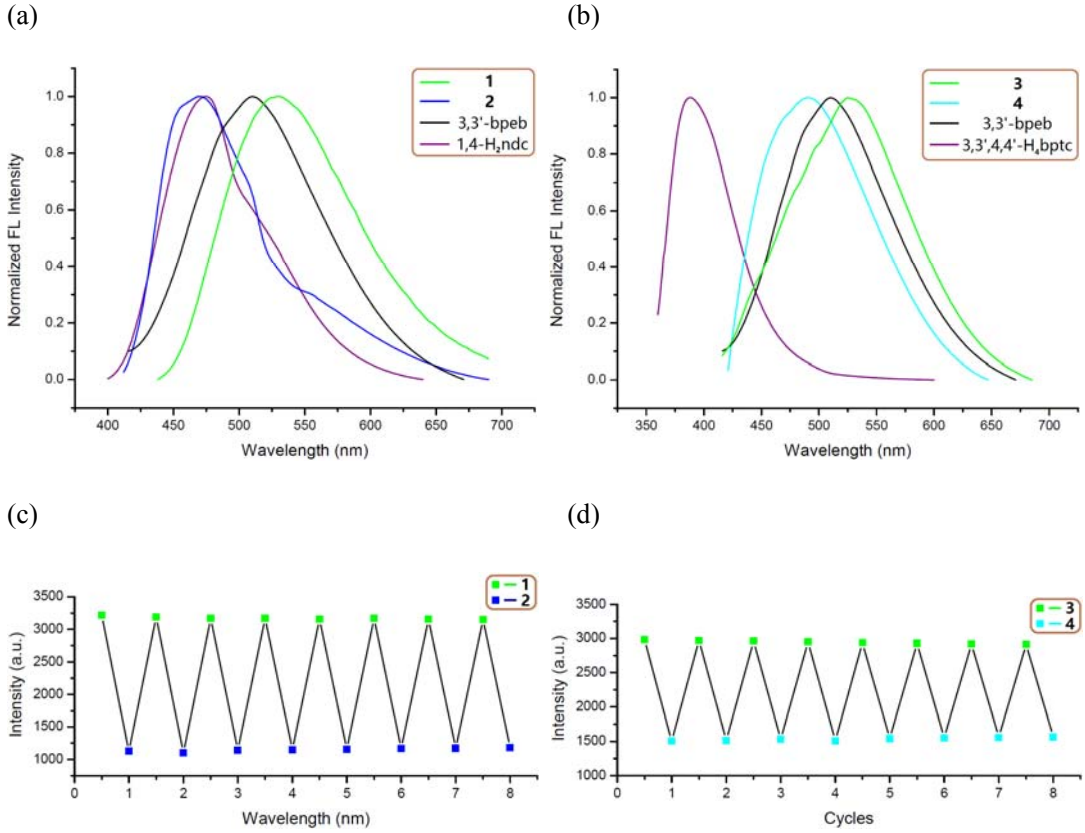

Fig. S13 (a) Normalized fluorescence spectra of **1**, **2**, 3,3'-bpeb and 1,4-H_2ndc in the solid state at ambient temperature. (b) Normalized fluorescence spectra of **3**, **4**, 3,3'-bpeb and 3,3',4,4'-H_4bptc in the solid state at ambient temperature. (c) The photoreaction reversibility of **1**. (d) The photoreaction reversibility of **3**. The fluorescence intensities for the experimental cycles were obtained by alternating UV irradiation and heating.

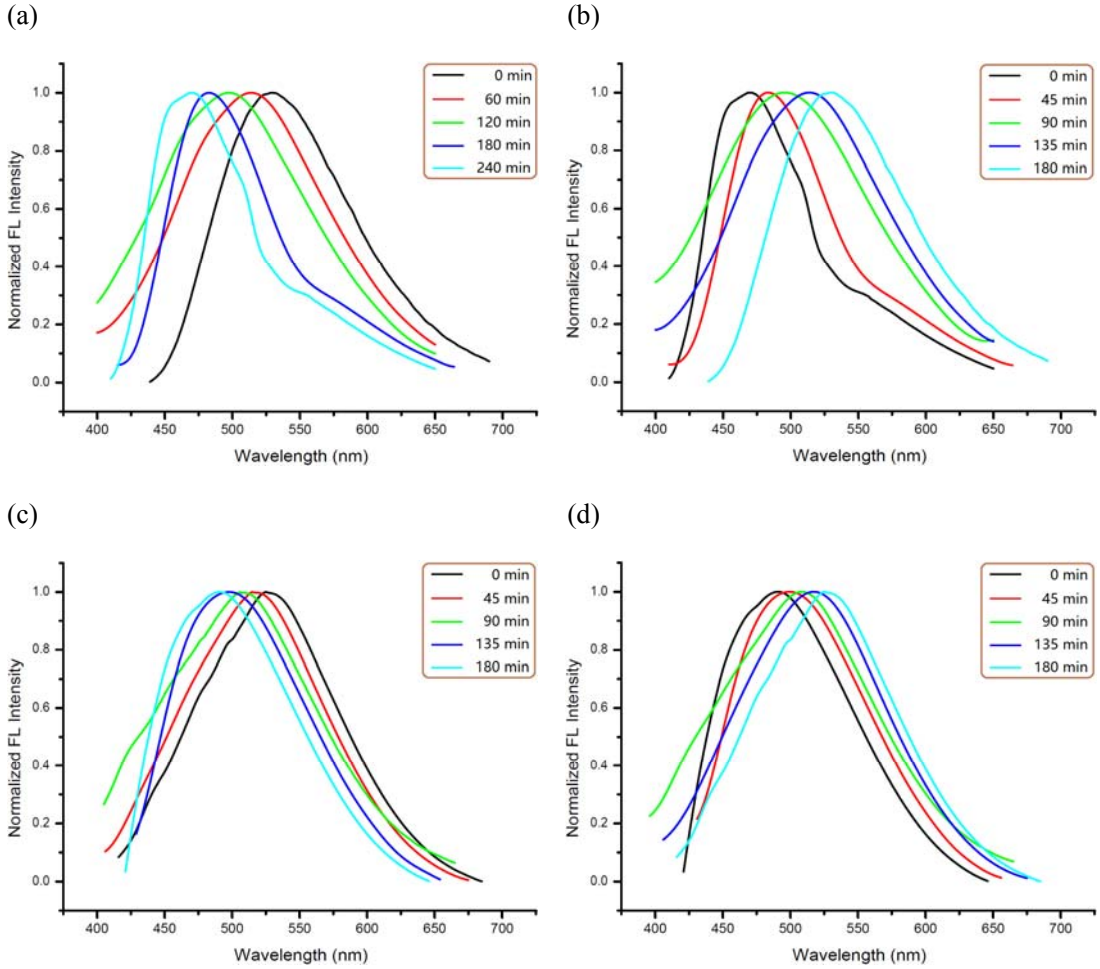

Fig. S14 (a) Normalized fluorescence spectra of **1** upon UV irradiation at different time intervals in the solid state. (b) Normalized fluorescence spectra of **2** upon heating at different time intervals in the solid state. (c) Normalized fluorescence spectra of **3** upon UV irradiation at different time intervals in the solid state. (d) Normalized fluorescence spectra of **4** upon heating at different time intervals in the solid state.

Noted: At each 60 min interval, a UV irradiated sample of **1** was collected for fluorescence measurement. As the time of UV irradiation was extended, the emission peak of the sample gradually exhibited a blue-shift from 529 to 514, 498, 483 and finally 471 nm. On the contrary, the fluorescence emission band of **2** showed a red-shift from 471 to 484, 496, 515 and 529 nm with increasing heating time at each 45 min interval. Along with the irradiated time increasing, the emission band of **3** displayed a blue-shift from 525 to 515 (45 min), 506 (90 min), 498 (135 min) and 491 nm (180 min). Similar to that of **2**, the emission band of the heating sample of **4** also represented a gradual red-shift. Accompanied by the increasing heating time at each 45 min interval, the sample showed emission bands at 491, 500, 509, 517 and 525 nm, respectively.

References

S1 G. M. Sheldrick, *SHELXL-2014*, *Program for Crystal Structure Refinement*, University of Göttingen, Göttingen, Germany, 2014.

S2 G. M. J. Schmidt, *Pure Appl. Chem.,* 1971, **27**, 647.